Improvement of EAF efficiency through an integrated control of scrap melting and slag characteristics

C. Mapelli, C. Corna, F. Magni

Several innovations have been introduced into the EAF system during the last decades. The improvement of energy efficiency and production rates are probably related to a correct integration of the different systems and to a correct design of the scrap charges as a function of the production rate, of the metal losses and of the energy consumption that are considered an optimal compromise to fulfil a correct economic balance for the melting, decarburation and dephosphoration operation. In order to achieve the aim of an energetic advanced model has been developed through the integration of the energy model of electric and chemical sources with the ones treating the metal bath oxidation and the foaming behaviour of the slags.

KEYWORDS:
steelmaking, melting, Electric Arc Fornace, scrap, slag, fume analysis

INTRODUCTION AND HISTORICAL OVERVIEW

In the last 40 years several technological innovations applied to Electric Arc Furnaces have allowed this kind of plant to become competitive in the production of both special and common carbon steels[1,2,3,4], starting from recycled steel scraps. This strong competitiveness has been reached by the progressive increasing of the installed power which can be erogated by electric current and the exploitation of the combustion processes.

Between 1965 and 1970 the need of increasing the production rates implied the introduction of oxygen injection featured by high flow rates, which increased the speed of steel oxidation and allowed the exploitation of the heat related to the presence of carbon combustion and the consequent formation of CO; 1975 saw the first application of the furnace walls cooling system by means of water cooled panels and these devices were introduced for mitigating the increasing thermal stresses on the refractory materials associated to the rising power provided by the arc.

One of the most significant innovations for Electric Arc Furnaces was introduced in 1978: the formation of foamy slags which shield the refractory walls against the radiation of the heating arc. These slags, obtained through carbon enrichment and oxygen injection, reach an average height of 0.3m, which is about three times the value assumed by non foamy slags. Such a thickness can be reached only by a correct managing in the injection of graphite powder and oxygen and it allows to work with long arc even when the whole scrap charge is melted, because the arc keeps itself submerged and surrounded by the slag, that absorbs most of the thermal radiation causing, a noticeable decrease in the thermal stresses on the walls and on the vault.

In 1979 the introduction of wall burners took place, in order to reach two operative aims: the exploitation of the chemical energy developed by the combustion of natural gas (CH4) and the heating of the cold spots along the furnace perimeter, related to the geometry of the electrodes. The effort of exploiting the energy coming from the chemical sources has known a strong intensification also during the last twenty years, especially for increasing the savings of electric energy, mainly in the countries featured by a strong dependence on hydro-carbides for the production of electric energy.

The latest technical innovation which deserves attention was introduced in 1983 and was represented by the Eccentric Bottom Tapping (EBT), which allowed fast tapping with no slag dragging or with a significant minimization of this phenomenon which can pollute the successive refining steps.

All these innovations drove to remarkable improvements in the process features: in 1965 the tap-to-tap time was approximately 3 hours with a specific electric consumption of 630kWh; nowadays the melting of 95 t of steel requires 35-40 minutes and the needed electric consumption is about half than 40 years ago (around 320kWh/t)[5,6,7].

In this context the role played by the features of the steel scraps has been usually considered as a secondary aspect, often evaluated on the basis of only empirical relations without the involvement of a systematic approach, so that in a lot of steelmaking unities the classification of the steel scrap is regarded as an important issue only during the commercial negotiation and not for the definition of the charged mixes that can maximize the productivity and even the metal losses during the melting operations. On the basis of such a historical landscape and of the EAF performances, the goal of an increasing performance can be reached through the correct integration of different aspects involved in the melting plant.

One of the aspects that can imply a favourable and significant efficiency improvement is associated to the correct scheduling of the energy supplying as a function of the scraps mix and of its change in heat transmission. Several interesting and rigorous studies have been focused on the changes of the physical properties of massive bulk steels[8], that certainly represent the theoretical basis for more complex modelling, but it is not directly suitable for the simulation in the arc furnace system. With the

Carlo MAPELLI
Dipartimento di Meccanica, Politecnico di Milano
(carlo.mapelli@polimi.it)

Cristian CORNA, Francesco MAGNI
Acciaieria Feralpi di Lonato

exception of the electrode automation, the other aspect strictly associated with the optimization of the power supply can be reached through a correct evaluation in the use of the scraps and by a correct controlling of the fume analysis that allows to monitor the efficiency of the combustion [9,10,11,12].
The integration of these aspects can represent a useful tool for increasing the efficiency of the melting process in terms of energy savings and decrease of the metal losses.

ASPECTS INTEGRATED WITHIN THE MODEL

Scrap Classification

Scrap mixes usually melted by means of Electric Arc Furnaces are made up of different scrap typologies; there is a European Reference Rule which classifies the different categories on the basis of their geometric features, paying a particular attention to the thickness. Moreover, the European Reference also fixes the maximum percentages of some alloying elements, such as copper and tin, which can be accepted in the steel scraps.
The scrap classification for the use as raw material for electric furnaces includes six different typologies, which can be defined on the basis of their geometric features:

- L (obtained from sheets): thin wastes of maximum thickness up to 3mm;
- D (obtained from demolition): old scraps characterized by big thickness (more than 5mm thick), including pipes and hollow sections of satisfactory thickness;
- T (obtained from turning wastes): homogeneous or mixed batches of carbon steels or cast irons of known origin, i.e. burrs from automatic steel processing are excluded from this category, due to the high sulphur content.

Scrap mixes usually contain even P (Heavy) and R (Gathered) materials, both of thickness smaller than 6mm, and PR (for scraps obtained from proler), made up of homogeneous elements of small sizes.
A significant attention should be paid to the effective scrap mix introduced into the furnace, especially if the steel mill has no control systems monitoring the geometrical features of the charged scrap. This represents a critical aspect, because as a matter of fact different scrap mixes can give rise to different material losses at the end of the melting process.
This is clearly understandable in Figure 1, where the results of a statistical analysis on all the melts carried out in 13 months for a 150 t EAF steelmaking unity are reported for an overall quantity of 1.45 Mt.
The graph shows the results ordered from the best month (minimum losses) to the worst one (maximum losses) as a function of the correspondent scrap mixes. Clearly the percentages of each scrap type are not constant and can vary in a significant range from one month to the following, but some statements can be put under evidence: the losses rise with the percentages of L and T scrap types charged in the EAF. This can be preliminary explained on the basis of the higher surface/volume ratio featuring the scrap types producing the highest losses: this geometric feature certainly drives to a higher volume of dirty and pollutant elements dragged into the furnace and to a more severe oxidation, especially in case of long permanence of the scraps in the stocking zones.

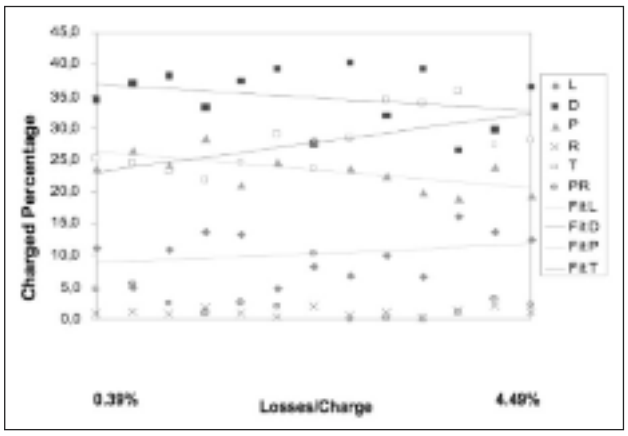

FIG. 1 ***Losses of the charged material as a function of the scrap categories (experimental data collected during the industrial trials).***

Perdite percentuali del materiale caricato in funzione della tipologia del rottame (I dati sperimentali sono stati registrati da operazioni fusorie realizzate con forno industriale).

Jet-slag-steel interaction

The study of the interaction among oxygen jet, steel and slag can be very difficult to be simulated dynamically, but it represents a fundamental aspect to achieve a better control and more regular practice of the oxygen injection. This aspect has important consequences on the oxidation of the steel bath, on the heat development after oxidation of the chemical elements contained in the bath and on the formation of the slags. The efforts performed by different authors have led to significant result using an approach based on dimensionless numbers to summarize the interaction among the involved fluids: injected gas, bubbles, steel and slag[13,14,15,16,17,18].
The problem is too complicated to be treated according the finite element approach whose performances are detrimentally affected by the numerical stability, so on the basis of the literature analysis seems to be more profitable a more stable approach based on the application of the dimensionless numbers.
The dimensionless number that will be taken into account[19,20,21,22,23,24,25,26,27]:

- Reynolds number

It is the ratio between the turbulent force and the viscous one and it can be used to estimate the features of the jet leaving the nozzle

$$\mathrm{Re} = \frac{u_0 d_0 \rho_0}{\mu_0} \quad (1)$$

or to evaluate the gas blowing around the bubbles developed within the slag

$$\mathrm{Re} = \frac{\rho v_r}{\mu} \quad (2)$$

- Froude number

Ratio of the inertial forces to gravitational ones and it can be used to represent lance blowing and possible bottom blowing

$$Fr = \frac{\rho_0 u^2}{g(\rho_0 - \rho)} \quad (3)$$

or it is used to estimate the inertial forces to gravitational ones produced by the gas jet on the foamed slag:

$$Fr = \frac{j_r^2}{gr} \quad (4)$$

- Capillary number

$$Ca = \frac{j_r \mu}{\sigma} \quad (5)$$

- Weber number

Ratio of momentum intensity to properties of liquid, then it is used to characterize droplet generation and it involves both jet

momentum and the properties of liquid from which the droplet are ejected

$$We = \frac{\rho_g u_g^2}{(\rho_l g \sigma_l)^{0.5}} \quad (6)$$

• Momentum number
Ratio between the jet momentum and the displaced liquid inertia

$$Mn = \frac{\rho_g A_n u^2}{\rho_l g x^3} \quad (7)$$

The use of the dimensionless numbers has been applied with success also for the study of the foaming behaviour[28,29,30,31,32,33,34,35,36].
The involvement of the formerly presented numbers allows the correct description of slag movement and the reliable interpretation of the slag foaminess as stated by Lotun et al.36). The concept of foaminess has been widely discussed and the conclusion is that it represents an idealization not supported by physical evidences. After the evaluation of several works and the comparison among the recorded experimental data found in literature, it is possible to conclude that the relation among the foam thickness and the average size of formed bubbles is:

$$\frac{H}{r} = kCa^{\alpha} \mathrm{Re}^{\beta} Fr^{\gamma} \quad (8)$$

where k=2617 α=−1.01 β=−1.74 γ=1.77.
Such a relation has been obtained through the application of the Buckingam Pi-theorem and so it is based on a robust approach. The obtained relation can be changed in:

$$\frac{H}{r} = 2617 \frac{\mu^{2.72} j_r^{2.78} \sigma^{2.01}}{\rho^{1.93} g^{2.72} r^{5.51}} \quad (9)$$

substituting the dimensionless number with the involved physical variables.
One of the most interesting conclusions is the role played by the surface tensions which is present at the numerator of the relation (9) and at a first sight this does not appear consistent from a thermodynamic point of view. This is due to the fact that the really significant variable is the ratio σ/ρ and the r value of the bubbles is strictly dependent on the surface tensions. The higher is the surface tensions the lower is the r value and so the slag is thicker (Figure 2, Figure 3), so the proposed relation does not contradict the basic thermodynamic principles and it can be applied to improve the performance of the simulation trial to be applied.
The consistency of the obtained results suggests that the proposed relation can be a useful tool for developing the model related to the slag-bath interaction in order to grant a more regular process.
The maximization of the foaminess improves the protection of the refractory walls that are shielded by the heat irradiated by the electric arc.

Oxidation and decarburization of the steel bath
Assumed that the refining period – of an EAF - is the time starting from the complete melting of the metallic charge until tapping, during this period the steel inside the furnace may be considered a liquid phase.
The injection of oxygen in the bath produces two main effects: the oxidation of the elements in solution with the steel, and the generation of heat that contributes to consequent electrical energy savings. Both these phenomena have to be described by a single model, since they are closely related.
The energy developed by the oxidation is valuable by the reaction enthalpy, once the number of reacting moles are known.

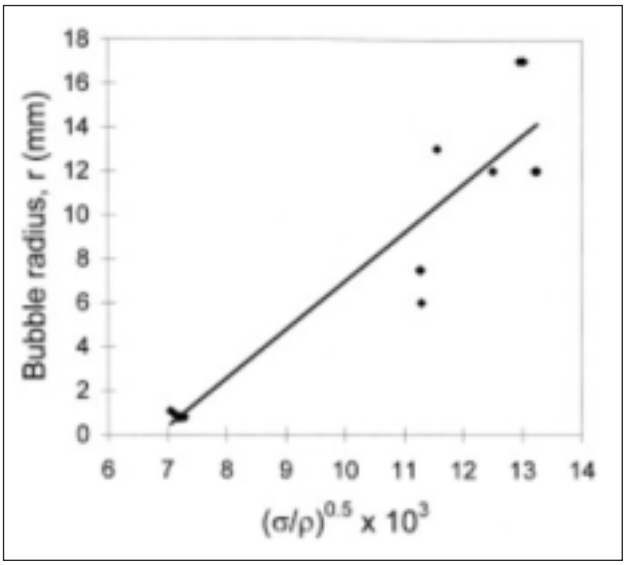

FIG. 2 ***Relation between σ/ρ and the bubble radius.***
Relazione tra il rapporto σ/ρ ed il raggio della bolla.

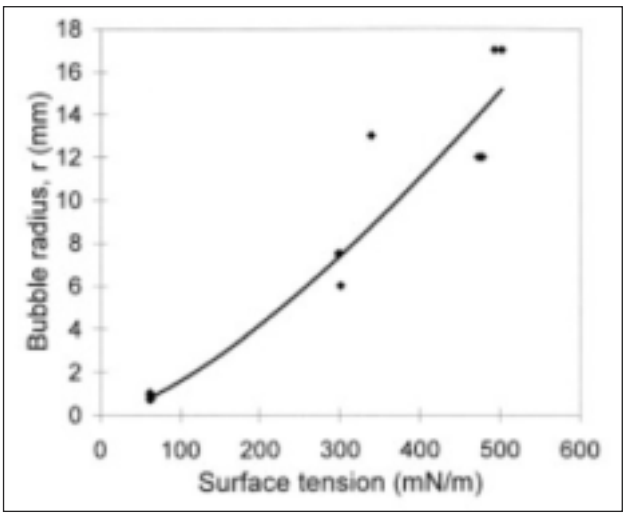

FIG. 3 ***Relation between surface tension and bubble radius.***
Relazione tra tensione superficiale e raggio della bolla.

Then the problem is to choose the chemical species oxidized in the bath and the calculation of the number of moles of a certain chemical species in solution that are oxidized by oxygen during a fixed time range.
The first point can be solved through the use of oxygen potentials.
Considering an oxidation reaction:

$$p[metal] + O_2 \rightleftarrows f(oxide) \quad (10)$$

According to Wagner theory the oxygen potential for this reaction is:

$$\Delta\mu_{O_2} = \Delta\mu^{\circ}_{O_2} - pRT\ln(a_{[metal]}) + fRT\ln(a_{oxide}) \quad (11)$$

To quantify the moles reacting, kinetics of the bath must be taken into account.
The diffusion laws give the number of the moles for a certain species that can move to the interface surface with the jet in Δ*t*. In terms of concentrations (ζ):

$$\zeta_i(\Delta t) = \zeta_i(t)\beta S \Delta t \quad (12)$$

where the transport constant β_i for each species can be calculated in turbulent conditions as:

$$\beta_i = \chi D_i^{\frac{1}{2}} u_\tau^{\frac{3}{2}} \rho_{steel}^{\frac{1}{2}} \sigma^{-\frac{1}{2}} \quad (13)$$

Since the difference between the diffusion constants for the elements dissolved in the steel bath are not significant for the description of the treated industrial case, only a single value for D_j has been used for all the species to simplify the computation:

$$D_i = 0.5 * 10^{-8} [m^2 s^{-1}] \quad (14)$$

The velocity u_τ is the average value of the steel velocity in correspondence of the cavity generated by the O_2 flow inside the bath. The velocity of steel can be calculated applying the momentum transfer between jet and bath:

$$v_{max}(x) = \sqrt{\frac{\rho_{O_2}}{\rho_{steel}}}\, v_{O_2}(x) \quad (15)$$

and u_τ is the average value over the range covered by the jet inside the bath:

$$u_\tau = \sqrt{\frac{\rho_{O_2}}{\rho_{steel}}} \left[\frac{1}{x_{max} - x_{steel}} \int_{x_{steel}}^{x_{max}} v_{ax}(x)\, dx \right] \quad (16)$$

The carbon injection and its integration in the model.
In the common melt shop practise and in the observed heats during the refining period of the melting operation, the carbon injection in the slag takes place too.
This is needed for some main reasons: first of all to avoid an excessive oxidation of the slag, to increase scrap yield and to promote the formation of foamy slag.
The role played by the carbon injection in the decarburisation phenomena has been studied in the same way operated for the oxygen injection through the use of kinetic factors ξ (each one different for each component of the slag)(Table 1):

$$\Delta\zeta_i = \xi_i \zeta_i \Delta t \quad (17)$$

and with the introduction of carbon potentials (analogous to the oxygen ones) for the reduction reactions in the slag:

$$\frac{1}{n}(Me_xO_y) + C \longrightarrow \frac{x}{n}[Me] + CO\uparrow \quad (18)$$

The reactions of SiO_2 and Al_2O_3 were neglected because their reduction potential is too high in the EAF process.
The moles of each species in the bath is completed by adding the contribute of the reduction from the slag and subtracting the oxidised moles of each species. In this way, combining in the same time interval the effect of the two phenomena of the oxygen and carbon injection, the model can estimate the composition of slag and steel bath (and the equilibrium between them) dynamically during the whole refining period. The total chemical energy developed is calculated by adding the enthalpies of oxidation for each oxidation reaction in an interval, and subtracting the reduction ones in the slag. The oxygen activity in the bath is constantly updated considering the equilibrium with the FeO in the slag:

$$\frac{[a_O]}{(a_{FeO})} = -\frac{6320}{T} + 2.765 \quad (19)$$

If the refining time is divided in several intervals, in each of them a thermodynamic description of the interface for each oxidation reaction can be performed through the use of the potential of oxygen.
Then, since the O_2 flow is known by imposing the technologic parameters of the process, the number of moles of oxidized elements can be evaluated starting from the one with the lowest potential and proceeding towards the higher potential ones. Only the free moles of oxygen left by each oxidation can react with the elements with higher potentials.
The amount of each species coming to the surface can be estimated. If there is oxygen left from the oxidation of the first element featured by the lowest oxygen potential it becomes available for the oxidation of the next lower element in the oxygen potential scales and so on.
On every time interval the activities of the elements at the surface can be evaluated considering the moles consumed in the former time step by the oxidation reactions and the diffusion laws. The temperature is evaluated at every time step by adding the heat developed by each reaction in terms of temperature difference in steel. This is true under the adiabatic hypothesis for the reaction surface:

$$\Delta E_j = \Delta H_j \left[m(t) - m(t + \Delta t) \right] \quad (20)$$

The enthalpy can be evaluated by:

$$\Delta H_j = \Delta H_j^0 + c_{p,j} \left[T - 298.15 \right] \quad (21)$$

where ΔH^0_j is the value of enthalpy at standard conditions for the j th reaction and cp is the specific heat at constant pressure. They can be easily evaluated according to Barin Knacke data (Table 1).
The sequence of this computation is developed for each time step taken into account to follow the thermo-chemical evolution of the considered system.
The decarburisation process can be limited by the flow of oxygen and by the carbon diffusion. When the oxygen consumes all the carbon available on the reaction surface and can oxidize also elements with higher potential, decarburisation is limited by the carbon diffusion to the interface. On the other hand, when the carbon consumes all the oxygen at the interface, the decarburization is controlled by the oxygen flow.
The application of the model in the condition of the observed industrial process shows that this transition takes place in the range of 0.2-0.4% (weight) of carbon in the bath. This matches the data presented in the bibliography about this topic.
The same can be observed for the other elements considered in the model. The described approach has been used to evaluate the chemical energy produced during the affination of the steel bath ($P_{chem\text{-}1}$).

Reaction	ΔH^0_j (kJ/molO_2)
$4/3\ Al + O_2 \rightarrow 2/3\ Al_2O_3$	-1088
$Si + O_2 \rightarrow SiO_2$	-882
$C + O_2 \rightarrow CO_2$	-366
$2C + O_2 \rightarrow 2CO$	-198
$2CO + O_2 \rightarrow 2CO_2$	-533
$1/2\ CH_4 + O_2 \rightarrow 1/2\ CO_2 + H_2O$	-372
$2/3\ CH_4 + O_2 \rightarrow 2/3\ CO_2 + 4/3\ H_2O$	-319
$2Fe + O_2 \rightarrow 2FeO$	-508

TAB. 1 ***Enthalpies associated to the considered oxidation reactions.***

Entalpie associate alle reazioni di ossidazione considerate.

Analysis of the off-gas

The analysis of the off-gas has been performed as a function of the formation of the foaming slag, the oxygen flow rate and the one of the methane. For the optimization of the process the me-

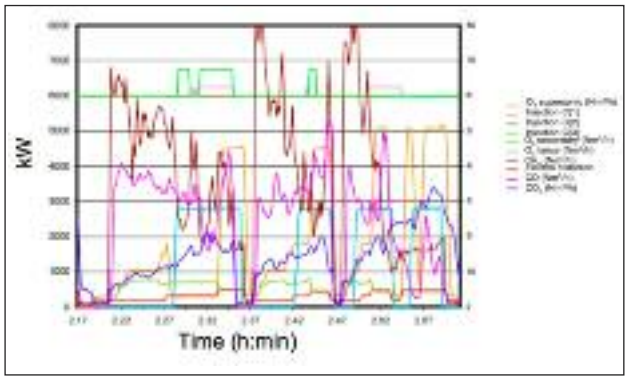

FIG. 4 ***Example of the main operative parameters related to a heat featured by a low specific electric energy consumption (310.92kWh/t).***

Esempio dei principali parametri operativi associati a una marcia fusoria caratterizzata da un basso consumo specifico di energia elettrica (310.92kWh/t).

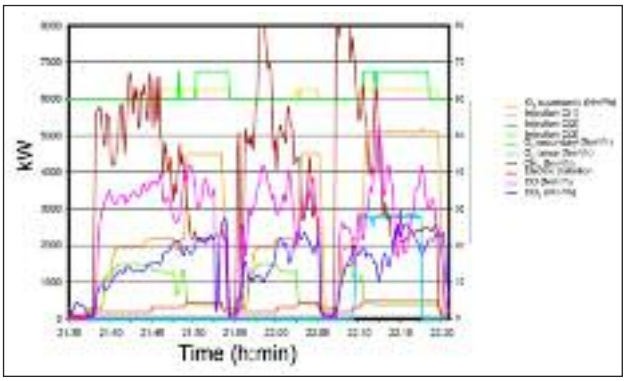

FIG. 6 ***Example of the main operative parameters related to a heat featured by high specific electric energy consumption (432.4kWh/t).***

Esempio dei principali parametri operativi associati a una marcia fusoria caratterizzata da un elevato consumo specifico di energia elettrica (432.4kWh/t).

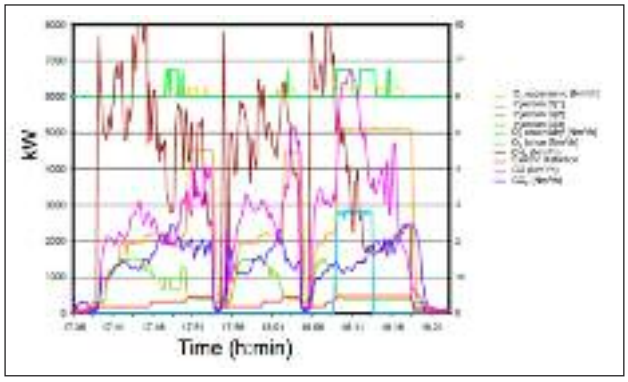

FIG. 5 ***Example of the main operative parameters related to a heat featured by a middle level of specific electric energy consumption (377.34kWh/t).***

Esempio dei principali parametri operativi associati a una marcia fusoria caratterizzata da un medio consumo specifico di energia elettrica (377.34kWh/t).

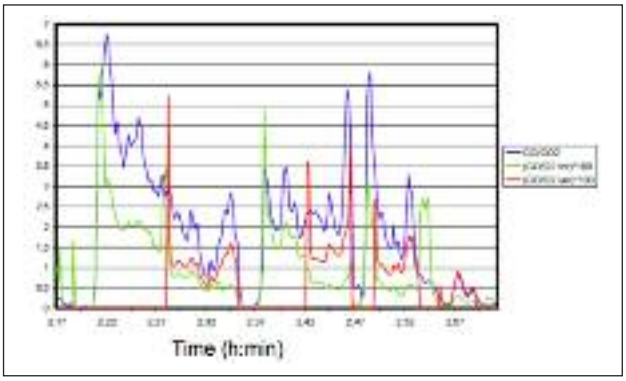

FIG. 7 ***Example of relation among CO, CO_2 and O_2 in a heat featured by a low specific electric energy consumption (310.92kWh/t).***

Esempio di relazione tra CO, CO_2 e O_2 in una marcia fusoria caratterizzata da un basso consumo specifico di energia elettrica (310.92kWh/t).

thane flow rate, the oxygen flow rate and the ratios CO/CO_2, $CO_2/O_{2\text{-tot}}$, $CO_2/O_{2\text{-inj}}$ have been taken into account. The increase of CO_2 fraction has to be reached in order to improve the energy efficiency, while an increase of CO flow rate points out a loss of the chemical energy that can be exploited.
A poor CO flow rate can suggest the possibility to increase the oxygen introduction avoiding the iron oxidation.

ANALYSIS OF THE MONITORED HEATS

The experimental activity has been performed in order to realize a correct validation of the model. 1200 heats have been analysed. The analysis has been made easier by the subdivision in 3 groups as a function of the consumption of the electric specific energy:

- Low Level: 310÷355kWh/t (Figure 4);
- Middle Level: 355÷400kWh/t (Figure 5);
- High Level: 400÷440kWh/t (Figure 6).

The increase of the CO_2 and the decrease of CO at the end of each EAF treatment is always associated to an increase of the oxigen flow rate (Figure 7, Figure 8, Figure 9). Moreover, the increase of the electric energy consumption is always associated to an unstable working of the oxigen-methane burners.

The electric distorsion is particularly evident at the beginnig of the melting step of the scrap after its charging.
An excessive fraction of CO in the EAF atmosphere is not desirable for the loss of the enthalpy developed by the complete oxidation to form CO_2 that cannot be exploited for melting.
The increase of the carbon injection seems to be strongly related with a significant increase of the electric energy consumption (Figure 10).
The most reliable hypothesis is that the added graphite powder could heat the slag but there is not any significant contribution to the increase of the bath thermal level and consuming a fraction of the introduced oxigen that is no longer available for enthalpy development that promotes the melting of the charged scrap.

MODEL

The treated aspects can be difficult to be integrated in a single model and the possible application of those results in a single tool can be difficult, especially if the automation system needs to robust and fast.
The obtained results can be summarized in a unique model based on the energy balance

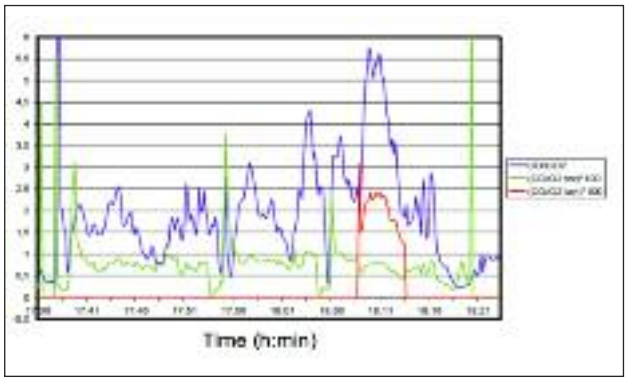

FIG. 8 ***Example of relation among CO, CO_2 and O_2 in a heat featured by a middle level of specific electric energy consumption (377.34kWh/t).***

Esempio di relazione tra CO, CO_2 e O_2 in una marcia fusoria caratterizzata da un medio consumo specifico di energia elettrica (377.34kWh/t).

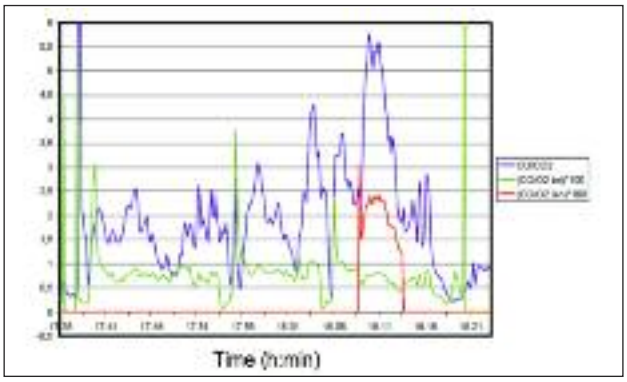

FIG. 9 ***Example of relation among CO, CO_2 and O_2 in a heat featured by a high level of specific electric energy consumption (432.44kWh/t).***

Esempio di relazione tra CO, CO_2 e O_2 in una marcia fusoria caratterizzata da un elevato consumo specifico di energia elettrica (432.44kWh/t).

$$\left[\eta_{elect}\frac{t_{powder-on}}{t_{tot}}P_{elect}+\eta_{injection}\frac{t_{injection}}{t_{tot}}P_{chem\_2}+\eta_{burner}\frac{t_{burner}}{t_{tot}}P_{chem\_2}+\right.$$
$$\left.+\eta_{burner}\frac{t_{burner}}{t_{tot}}P_{chem\_2}+\eta_{lance}\frac{t_{lance}}{t_{tot}}P_{lance}\right]t_{tot}=\rho c_p\left(T_{fin}-T_{in}\right) \quad (22)$$
$$+H_{loss}+f_{liq}\lambda_{melt}$$

the input data of the model are the different action times (tx), P_{elect}, the enthalpy reaction data associated to the oxidation reactions, the final temperature of the bath and the initial temperature, while t_{tot} is the tap to tap overall time and it can be isolated and computed in order to evaluate the melting and the decarburation EAF period. Because of the heat conductivity varies as the melting goes, an incremental time procedure is needed to take into account the progressive variation of the physical ruling variables. These variables are involved in the computation through the variation of the efficiency in heat transfer (η_x) that has been estimated through the experimental measurement. Thus, the equation takes another form:

$$\sum_{n}\left[\eta^{(n)}_{elect}\frac{\Delta t^{(n)}_{powder-on}}{\Delta t^{(n)}}P_{elect}+\eta^{(n)}_{injection}\frac{\Delta t^{(n)}_{injection}}{\Delta t^{(n)}}P^{(n)}_{chem\_2}+\right.$$
$$\left.+\eta^{(n)}_{burner}\frac{\Delta t^{(n)}_{burner}}{\Delta t^{(n)}}P^{(n)}_{chem\_2}+\eta^{(n)}_{lance}\frac{\Delta t^{(n)}_{lance}}{\Delta t^{(n)}}P^{(n)}_{lance}\right]t \quad (23)$$
$$-H^{(n)}_{loss}=M_{steel}c_p\left(T_{fin}-T_{in}\right)+f_{liq}\lambda_{melt}$$

The value of $P^{(n)}_x$ varies as a function of the energy provided to the steel bath and on the heat loss ($H^{(n)}_{loss}$) imposed by the operational conditions.

This relation can be considered at a specific instant (i) since the beginning step:

$$\sum_{n}\left[\eta^{(n)}_{elect}\frac{\Delta t^{(n)}_{powder-on}}{\Delta t^{(n)}}P_{elect}+\eta^{(n)}_{injection}\frac{\Delta t^{(n)}_{injection}}{\Delta t^{(n)}}P^{(n)}_{chem\_2}+\right.$$
$$\left.+\eta^{(n)}_{burner}\frac{\Delta t^{(n)}_{burner}}{\Delta t^{(n)}}P^{(n)}_{chem\_2}+\eta^{(n)}_{lance}\frac{\Delta t^{(n)}_{lance}}{\Delta t^{(n)}}P^{(n)}_{lance}\right]t \quad (24)$$
$$-H^{(n)}_{loss}=M^{(n)}_{steel}c_p\left(T^{(n)}-T_{in}\right)+f_{liq}\lambda_{melt}$$

The efficiency associated to each energy term is a function of the internal energy supplied to the steel bath and the possible heat losses (especially the ones related to heat dispersion from the walls, the fumes and the slag mass to be maintained at the correct thermal levels):

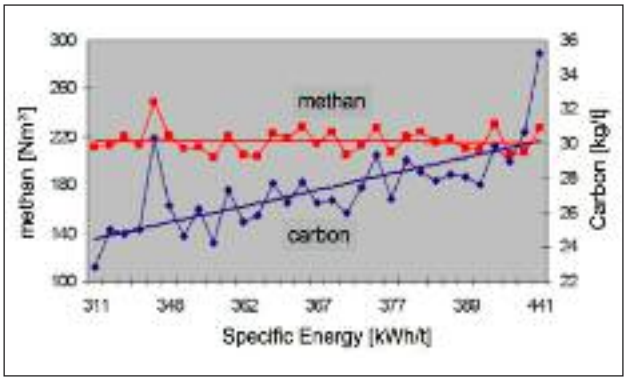

FIG. 10 ***Example of several analysed heats featured the same level of specific methane consumption and different levels of specific carbon addition and specific electric energy consumption.***

Relazione osservata sperimentalmente in marce fusorie industriali tra aggiunta di polverino grafitico, consumo di metano e consumo specifico di energia elettrica.

$$\eta_{elect}=0.725\frac{\rho_{apparent-scrap}+\left(\rho_{scrap}-\rho_{apparent-scrap}\right)\left[\rho_{steel}c_p\left(T^{(i)}-T_{in}\right)\right]/\left[\rho_{steel}c_p\left(T_{fin}-T_{in}\right)\right]}{\rho_{scrap}} \quad (25)$$

$$\eta_{injection}=0.45\frac{\rho_{apparent-scrap}+\left(\rho_{scrap}-\rho_{apparent-scrap}\right)\left[\rho_{scrap}c_p\left(T^{(i)}-T_{in}\right)\right]/\left[\rho_{scrap}c_p\left(T_{fin}-T_{in}\right)\right]}{\rho_{steel}} \quad (26)$$

$$\eta_{burner}=0.38\frac{\rho_{apparent-scrap}+\left(\rho_{scrap}-\rho_{apparent-scrap}\right)\left[\rho_{scrap}c_p\left(T^{(i)}-T_{in}\right)\right]/\left[\rho_{scrap}c_p\left(T_{fin}-T_{in}\right)\right]}{\rho_{steel}} \quad (27)$$

$$\eta_{lance}=0.35\frac{\rho_{apparent-scrap}+\left(\rho_{scrap}-\rho_{apparent-scrap}\right)\left[\rho_{steel}c_p\left(T^{(i)}-T_{in}\right)\right]/\left[\rho_{steel}c_p\left(T_{fin}-T_{in}\right)\right]}{\rho_{steel}} \quad (28)$$

The losses of the developed heat is partially included in the efficiency heat transfer coefficient (η_x), but the heat dispersion through the refractory walls and the water cooled modules have to be taken into account. In the terms $P_{chem\text{-}1}$ and $P_{chem\text{-}2}$ all the combustion reactions have to be taken into account and these include also the combustion due to the carbon injection to promote and maintain the foaming slag (2nd paragraph).

$$H_{loss}^{(n)} = M_{slag}^{(n)} c_{p\_slag} (T^{(n)} - T^{(n-1)}) + \frac{k_{slag\_formed}}{H^{(n)}} (T_{slag} - T_{furnace}) 2\pi r_{furnace} + M_{wp} c_{p\_wp} (T_{wp}^{(n)} - T_{wp}^{(n-1)}) + T_{water}^{(n)} \Delta T_{water}^{(n)} M^{(n)} + H_{open\_door} M^{(n)} \quad (29)$$

The terms involved in the loss term are related to the heat needed to maintain the slag hot (inserted CaO and formed slag), heat transfer through the slag, heating of the refractory walls and the heat absorbed by the water cooled panel, where ΔT_{water} represents the measured difference in the thermal temperature between the inlet section and the outlet one. The last term is associated to heat loss due to the opening of the furnace for the charge of the different baskets. This last term should be divided in the discretized elements.

DISCUSSION AND CONCLUSIONS

The energy model has shown a good agreement with the experimental data. It is interesting the role played by the flow rate of the water cooled panels and the one covered by the graphite powder injection needed for forming and maintaining the foamed slag.
It is interesting that some terms can have certainly favourable defect, but also possible drawbacks.

- the oxidation of iron and alloying elements produces also an amount of slags that have to be maintained at the correct thermal level although the low heat conductivity and the high specific heat of the oxide compounds;
- although the carbon injection introduced to permit the formation of foaming slag represents a consolidated practice, this action has to be reasonably contained. Actually, the implementation of the developed incremental energy model has pointed out a carbon oxidation whose enthalpy is not efficiently transferred to the steel bath and related protection of the oxidation of iron and alloying elements that react in a lower fraction. This phenomenon is evident also in the fume analysis and in the evaluation of the electric energy in presence of an excessive presence of graphite addition;
- the described situation suggests that the useful and favourable formation of a foamed slag featured by significant height should be promoted by also alternative method, i.e. gas introduction and bubble formation from the bottom of the EAF furnace. Actually, a good a highly foamed slag (350-450mm) can perform a favourable insulating effect that has been taken into account in the decreasing of H_{loss}.

REFERENCES

1. W. Nicodemi: Siderurgia, processi e impianti, Associazione Italiana di Metallurgia, Milano (1994);
2. L.Brooks, N.Provatas: http://mse.mcmaster.ca/graduate/seminar/2005/702_Seminar_JianghuaLi_November_2005.pdf
3. D. R. Poirier, G. H. Geiger: Transport phenomena in materials science, (1994), 398.
4. X. Cheng, U. Muller: Int. J. Heat and Mass Transfer, 41(1998), 1681.
5. F. Memoli, C. Mapelli, P. Ravanelli, M. Corbella: ISIJ International, 44(2004), 9, 1511.
6. F. Memoli, C. Mapelli, P. Ravanelli, M. Corbella: ISIJ International, 44(2004), 8, 1342
7. C. Mapelli, S. Baragiola: Ironmaking and Steelmaking, 33(2006), 5, 379.
8. B. E.Launder, D. B. Spalding: Computer methods in applied mechanics and engineering, (1974), 269.
9. D. R. Gaskell: An introduction to transport phenomena in materials engineering, Macmillian Publications, (1992), 614.
10. R. I. L. Guthrie: Engineering in Process Metallurgy, Oxford Science Publications, (1993), 296.
11. P. Gardin, C. Soide, A. Dez and I. Guillaume: Ironmaking Steelmaking, 19(1992), 306.
12. E. H. McIntyre and E. R. Landry: Iron Steelmaker, 20(1993), 61.
13. H. Jourbet: Proc. 6th Int. Conf. on Molten Salts, Fluxes and Slags, Royal Inst. of Tech., Stockholm, and Helsinki Univ. of Tech., Helsinki, (2000).
14. V. Okhotskii and A. Schramko: Steel USSR, 20 (1990), No. 7, 317.
15. J. Cui, W. Yang and C. Zheng: Iron Steelmaker, 27 (2000), July, 39.
16. R. Eade: New Steel, 13 (1997), Oct., 50.
17. F. Xiao, Y. Liang, J. Li and J. Yu: J. Wuhan Univ. Sci. Technol., 24 (2001), No. 2, 122.
18. C. Messina: Iron Steel Eng., 73 (1996), May, 17.
19. F. Zhao: Shanghai Met., 21 (1999), No. 5, 40.
20. J. Waing and Z. Liu: Steelmaking (China), 16 (2000), No. 4, 6.
21. J. Xie: Res. On Iron Steel (China), (2001), 10.
22. K. Goodson, N. Donaghy and R. Russell: Iron Steelmaker, 22 (1995), June, 31.
23. D. Yue, J. Zheng and Y. Liu: Proc. Chinese Soc. Materials Meeting, CSM, Beijing, (2003), 273.
24. L. Zhong, Y. Zhu, X. Yao, D. Lu, B. Hu and M. Shu: J. Iron Steel Res. (China), 14 (2002), 74.
25. M. Luomala, T. M. J. Fabritius, E. O. Virtanen, T. P. Siivola, T. L. J. Fabritius, H. Tenkku and J. J. Härkki: ISIJ Int., 42 (2002), 1219.
26. M. Luomala, E. Vitanen, P. Mure, T. Sivola, T. Fabrikas and J. Härkki: Steel Res., 73 (2000), 9.
27. A.Garg and K. Peaselee: Proc. 80th Steelmaking Conf., ISS/AIME, Warrendale, PA, (1997), 87.
28. Pajotskii, R. Behera, A. Sarangi and S. Misra: Iron Steel Int., 55 (1982), No. 1, 27.
29. S. Koria and K. Lange: Metall. Trans. B, 15B (1984), 109.
30. K. Li: J. Iron Steel Inst., 196 (1960), 275.
31. A.Chatterjee and A. Bradshaw: J. Iron Steel Inst., 208 (1972), 179. J. Park and C. Ha: Rev. Metall., Cah. Inf. Tech., 97 (2000), 729.
32. B.Roth, M. Peter, M. Juhart and K. Koch: Steel Res., 70 (1999), 502.
33. A.He: Steelmaking (China), 17 (2001), No. 4, 22.
34. S. Paul and D. Ghosh: Metall. Trans. B, 17B (1986), 461.
35. A.Sakai, J. Tani, K. Yamada, K. Maya and S. Fugagawa: Steelmaking Conf. Proc., ISS/AIME, Warrendale, PA, (1994), 61.
36. Luton, L.Pilon; ISIJ Int. 45 (2005), 6, 835-840.
37. I. Barin, O.Knacke: Thermochemical properties of inorganic substances, Sprinter-Verlag Berlin Heidelberg New York, Verlag Stahleisen m.b.H. Düsseldorf (1973).

Abstract

Miglioramento delle prestazioni del forno elettrico ad arco mediante un controllo integrato del tipo di rottame e delle caratteristiche della scoria

Parole chiave: produzione di acciaio, forno elettrico ad arco, rottame, scoria, analisi dei fumi

Diverse innovazioni sono state introdotte nei forni ad elettrico durante gli ultimi decenni. L'incremento dell'efficienza energetica e dei tassi produttivi sono stati gli obiettivi che hanno guidato questa evoluzione. Un'ulteriore incremento dell'efficienza dei sistemi fusori si rivelerà probabilmente legato ad una corretta integrazione degli aspetti relativi alla tipologia del rottame caricato, alla cor-

retta modulazione dell'energia elettrica e chimica e alla stabilizzazione delle scorie schiumose. Le perdite di massa metallica caricata risultano strettamente correlate con la morfologia e tipologia del rottame (Fig. 1), mentre la stabilizzazione della scoria schiumosa può essere correttamente studiata attraverso l'utilizzo del teorema di Buckingham (Figg. 2, 3). Un modello energetico è stato sviluppato per rendere conto delle variazioni del consumo specifico di energia elettrica al variare delle condizioni di esercizio (Figg. 4, 5, 6) a cui corrispondono diversi andamenti dei fenomeni di ossidazione e di sviluppo delle specie chimiche ad essi associati (Figg. 7, 8, 9). Le rilevazioni sperimentali ed il modello matematico confermano che l'introduzione eccessiva di polverino grafitico può risultare del tutto controproducente a causa dell'assorbimento di calore che tende a diminuire lo sviluppo di calore del sistema e quindi a spostare l'equilibrio verso l'ossidazione del ferro (Fig. 10).

List of symbols

a	Activity
A_n	nozzle area (m^2)
β_i	Transport coefficient (m/s)
c_p	specific heat of steel at constant pressure [680 $Jkg^{-1}K^{-1}$]
$c_{p\ slag}$	specific heat of the refractories [J/kgK]
c_p	Specific heat of the steel bath [J kg^{-1} K^{-1}]
$c_{p,\ steel}$	Specific heat of the steel bath [J kg^{-1} K^{-1}]
$c_{p,\ ref}$	Specific heatof the refractories [J kg^{-1} K^{-1}]
Ca	capillarity number
d_0	diameter of the injecting lance (m)
D_i	Diffusion constant in liquid steel for a given species [m^2/s]
E_j	Energy associated with the heat development [J]
Fr	Froude number
g	gravity acceleration (m/s^2)
γ	Specific heat ratio of a gas
η_{elect}	efficiency of heat transfer from the electric arc to the charged material
$\eta_{injection}$	efficiency of heat transfer from the oxidation reaction to the charged scrap during the decarburation period
η_{burner}	efficiency of heat transfer from the combustion of methane to the charged scrap
η_{lance}	efficiency of the heat transfer from the oxidation combustion produced by the oxigen lance to the charged scrap
h_{steel}	Vertical depth in the bath calculated at a certain ascissa [m]
H	Enthalpy [J mol^{-1}]
H_{loss}	Overall loss of the enthalpy [J]
H_{open}	Enthalpy lost during the fornace opening [J]
He	Height of the exit transversal section of the nozzle above the plane level of the bath [m]
ΔH^0	Enthalpy at standard conditions [J mol^{-1}]
j_r	reduced surface gas velocity (m/s)
Re	Reynolds number
u_0	gas velocity at the outlet section of the nozzle (m/s)
u_g	velocity of the gas jet (m/s)
u	gas velocity (m/s)
u_τ	average velocity of steel in correspondence of the jet surface [m/s]
μ_g	viscosity of the gas phase (Pas)
μ	viscosity (Pas)
ξ_i	proportional kinetic constant for oxide *i* slag [s^{-1}]
ζ_i	Concentration of moles of the specie i [mol m^{-3}]
r	average radius of the bubble contained in the foam (m)
ρ	density (kg/m^3)
ρ_g	density of the gas phase(kg/m^3)
ρ_l	density of the liquid phase (kg/m^3)
ρ_{02}	Jet density [kg/m^3]
$\rho_{scrap\text{-}apparent}$	Apparent density of the charged scrap [kg/m^3]
ρ_{in}	Density of the injected gas at the entry transversal section of the nozze [kg/m^3]
ρ_{steel}	Density of the liquid steel [kg/m^3]
σ	surface tension (Nm)
σ_l	surface tension between the gas and the liquid phases (Nm)
x	depth of cavity (m)
We	Weber number
λ_{melt}	melting enthalpy [270kJ kg^{-1}]
F_{water}	flow rate of the cooling water [kg/m^2s]
f_{liq}	melted fraction of the scrap
t	time [s]
T	temperature [K]
χ	Proportional kinetic constant for bath
$(\cdot)$	Concentration of an oxide in the slag [mol m^{-3}]
$\Delta\mu^*_{02}$	Oxygen standard potential [kJ/mol]
$\Delta\mu_{02}$	Oxygen potential [kJ/mol]
ΔT_{water}	Temperature difference of the water between the inlet section outlet one of the cooling system [K]
Δt	Time interval [s]
$k_{slag\ foamed/unfoamed}$	Slag conductivity in foaming or non foaming condition [W/mK]
L_p	Coherence length [m]
λ_{melt}	latent heat melting [272kJ/kg]
$m(t)$	moles of the oxidized species at the time (t)
m_{Fe}	moles of Fe in the bath [mol]
M_{ref}	mass of the refractory [kg]
M_{slag}	mass of the formed slag [kg]
R	perfect gas universal constant [$Jmol^{-1}K^{-1}$]
S	surface of the interface between the gas jet anf the liquid steel [m^2]
T_{in}	initial temperature [K]
T_{fin}	final temperature [K]
$T^{(n)}_{ref}$	temperature of the refractories at time step (n) [K]
$T^{(n)}$	temperature of the steel after (n) discretized step
v_{steel}	average velocity of the steel[m/s]
v_{02}	velocity of the oxigen jet[m/s]
v_{ax}	axial velocity (component of the velocity along the axis of symmetry of the jet) [m/s]
x	axial coordinate taken from the nozzle outlet [m]
x_{max}	abscissa where the axial velocity is zero [m]
x_{steel}	abscissa of the intersection of the jet axis with the plane of the bath surface [m]
f,q,n	stoichiometric coefficients